Insights on the Estimation Performance of GNSS-R Coherent and Noncoherent Processing Schemes

Article *in* IEEE Geoscience and Remote Sensing Letters · May 2021

DOI: 10.1109/LGRS.2021.3079579

3 authors:

Lorenzo Ortega Espluga
Institut Polytechnique des Sciences Avancées
43 PUBLICATIONS **127** CITATIONS
SEE PROFILE

Jordi Vilà-Valls
Institut Supérieur de l'Aéronautique et de l'Espace (ISAE)
129 PUBLICATIONS **815** CITATIONS
SEE PROFILE

E. Chaumette
Institut Supérieur de l'Aéronautique et de l'Espace (ISAE)
174 PUBLICATIONS **1,039** CITATIONS
SEE PROFILE

Insights on the Estimation Performance of GNSS-R Coherent and Non-Coherent Processing Schemes

Lorenzo Ortega, Jordi Vilà-Valls, *Senior Member, IEEE*, Eric Chaumette, *Member, IEEE*

***Abstract*—Parameter estimation is a problem of interest when designing new remote sensing instruments, and the corresponding lower performance bounds are a key tool to assess the performance of new estimators. In Global Navigation Satellite Systems reflectometry (GNSS-R), a non-coherent averaging is applied to reduce speckle and thermal noise, and subsequently the parameters of interest are estimated from the resulting waveform. This approach has been long regarded as suboptimal with respect to the optimal coherent one, which is true in terms of detection capabilities, but no analysis exists on the corresponding parameter estimation performance exploiting GNSS signals. First, we show that for certain signal models, both coherent and non-coherent Cramér-Rao bounds are equivalent, and therefore, any maximum likelihood estimation coherent/non-coherent combination scheme is efficient (optimal) at high signal-to-noise ratios. This is validated for an illustrative GNSS-R estimation problem. In addition, it is shown that considering the joint delay/Doppler/phase estimation problem, the non-coherent performance for the delay is still optimal, which is of practical importance for instance in altimetry applications.**

***Index Terms*—Cramér-Rao bound, coherent/non-coherent processing, maximum likelihood estimation, GNSS, GNSS-R.**

I. Introduction

PARAMETER estimation is a fundamental problem for any Earth observation application, such as Global Navigation Satellte Systems (GNSS), radar or GNSS reflectometry (GNSS-R) [1]–[3], where the first stage of the receiver is in charge of estimating the time-delay and the Doppler of the received signal. In addition, phase estimation is required in some applications such as precise navigation [1] or new precise GNSS-R approaches [4]–[6]. In any case, a key question on the receiver design is whether it is possible to use optimal coherent signal processing schemes, or if in contrast non-coherent processing strategies must be accounted for.

In conventional GNSS-R (cGNSS-R) receivers, the direct signal processing implements a coherent maximum likelihood estimatior (MLE) processing to estimate the direct signal delay, Doppler and phase [1], [4], which are used to feed the processing of the reflected signal. In this context, the received signal after reflection over a surface is spread in time and Doppler because of the scattering on the surface, and the relative motion between the transmitter and the receiver. Regarding the surface, i) over the ice the scattered signal is almost a specular reflection with a strong coherent signal component, ii) over the ocean the so-called glistening zone [3] is significantly increased and the incoherent signal component is much more important than the coherent one, and iii) over land, both coherent and non-coherent components appear [7]. The resulting function after correlation is the so-called delay-Doppler map [8]. This correlation is obtained over a coherent integration time, which must be shorter than the coherence time of the noisy scattered signal [3]. Subsequently, a non-coherent processing is performed to reduce speckle and thermal noise, and obtain the final GNSS-R product, which is given by a specific point of the resulting waveform [9], [10].

Then, for GNSS-R it is fundamental to obtain the estimation performance limits in the mean square error (MSE) sense of both coherent and non-coherent schemes, an information brought by the corresponding Cramér-Rao lower bound (CRB) [11], which gives an accurate MSE estimation of the MLE in the asymptotic region, i.e., high signal-to-noise (SNR) regime of the Gaussian conditional signal model (CSM) [12], [13]. In the GNSS literature, non-coherent (post-detection integration (PDI)) processing schemes have been mainly analyzed in the context of signal detection [14], [15], for which it is known that in the absence of data bits the coherent processing is the optimal one, and any other PDI technique is suboptimal. In the GNSS-R literature, the coherency of the reflected signal, the impact of the coherent integration time and the specular point re-tracking have been addressed [16]–[19]. To the best of the author's knowledge, no comparative analysis (neither in GNSS nor in GNSS-R) for the coherent and non-coherent estimators' performance exists from an estimation standpoint.

In this contribution we first show that for certain single source CSMs both coherent and non-coherent CRBs are equivalent, then in this case any coherent/non-coherent MLE is efficient at high SNR. This result is validated for a GNSS-R delay estimation problem, of interest for instance in altimetry applications. Secondly, we provide the corresponding analysis for a more general case where the Doppler is not the same for both signals, and therefore, it must also be estimated for the reflected signal. In that perspective, results show that the non-coherent delay estimation is still optimal, but the Doppler estimate reaches the CRB only for non-coherent schemes involving a squaring detector. Therefore, these schemes must be considered to correctly use the carrier phase. The results are obtained for a GPS L1 C/A signal, for which the minimum coherent processing time is the so-called pseudorandom noise (PRN) code duration equal to 1 ms. In practice, the maximum coherent correlation time must be shorter than the signal coherency time [3], which limits the use of coherent schemes. Data bits are not a problem if correctly handled [16], [20], as well as Doppler offsets if using a proper re-tracking [17].

L. Ortega is with University of Toulouse TéSA/ISAE-SUPAERO, Toulouse, France; J. Vilà-Valls and E. Chaumette are with University of Toulouse, ISAE-SUPAERO, Toulouse, France; This research was partially supported by TéSA and the DGA/AID projects (2019.65.0068.00.470.75.01, 2018.60.0072.00.470.75.01).

II. CRBs and Estimators for Coherent/Non-Coherent Processing Schemes

A. From Multiple to Single Source

Let us consider the well known CSM [12] with M sensors (snapshots), D signals sources, P unknown parameters for each source and T independent and identically distributed (i.i.d.) realisation of noise $\mathbf{n}_t$,

$$\mathbf{x}_t = \mathbf{A}\left(\boldsymbol{\Theta}\right)\mathbf{s}_t + \mathbf{n}_t,\ 1 \leq t \leq T, \tag{1}$$

with $\mathbf{x}_t^\top = \left(x_1\left(t\right), \ldots, x_M\left(t\right)\right)$, $\mathbf{n}_t^\top = \left(n_1\left(t\right), \ldots, n_M\left(t\right)\right)$, complex amplitudes $\mathbf{s}_t^\top = \left(s_1\left(t\right), \ldots, s_D\left(t\right)\right)$, $\mathbf{A}\left(\boldsymbol{\Theta}\right) = \left[\mathbf{a}\left(\boldsymbol{\theta}_1\right)\ \ldots\ \mathbf{a}\left(\boldsymbol{\theta}_D\right)\right]$ with $\mathbf{a}\left(\boldsymbol{\theta}_i\right)$ a generic i-th received signal model, $\boldsymbol{\Theta} = \left[\boldsymbol{\theta}_1\ \ldots\ \boldsymbol{\theta}_D\right] \in \mathbb{R}^{P\times D}$ and $\mathbf{n}\left(t\right) \sim \mathcal{CN}\left(\mathbf{0}, \sigma^2\mathbf{I}\right)$. Then, the MLE $\widehat{\boldsymbol{\Theta}}$ of $\boldsymbol{\Theta}$ is the given by [21, (4.53)]

$$\begin{aligned}\widehat{\boldsymbol{\Theta}} &= \arg\left\{\min_{\boldsymbol{\Theta}}\left\{\sum_{t=1}^{T}\mathbf{x}_t^H\boldsymbol{\Pi}^{\perp}_{\mathbf{A}(\boldsymbol{\Theta})}\mathbf{x}_t\right\}\right\}\\ &= \arg\left\{\max_{\boldsymbol{\Theta}}\left\{\sum_{t=1}^{T}\mathbf{x}_t^H\boldsymbol{\Pi}_{\mathbf{A}(\boldsymbol{\Theta})}\mathbf{x}_t\right\}\right\},\end{aligned} \tag{2}$$

where given $S = span\left(\mathbf{A}\right)$ the linear span of the set of the column vectors of matrix $\mathbf{A}$, $\boldsymbol{\Pi}_{\mathbf{A}} = \mathbf{A}\left(\mathbf{A}^H\mathbf{A}\right)^{-1}\mathbf{A}^H$ is the orthogonal projection over S, and $\boldsymbol{\Pi}^{\perp}_{\mathbf{A}} = \mathbf{I} - \boldsymbol{\Pi}_{\mathbf{A}}$.

On the other hand, the CRB associated to $\boldsymbol{\Theta}$ is [22, (2.18)]

$$\begin{aligned}&\mathbf{CRB}_{\boldsymbol{\Theta}} = \mathbf{F}_{\boldsymbol{\Theta}}^{-1}, \mathbf{F}_{\boldsymbol{\Theta}} = \frac{2T}{\sigma^2}\mathrm{Re}\left\{\boldsymbol{\Phi}\left(\boldsymbol{\Theta}\right)\odot\left(\widehat{\mathbf{R}}_{\mathbf{s}}^T\otimes\mathbf{1}_{P,P}\right)\right\},\\ &\boldsymbol{\Phi}\left(\boldsymbol{\Theta}\right) = \left[\begin{array}{ccc}\frac{\partial\mathbf{a}(\boldsymbol{\theta}_1)}{\partial\boldsymbol{\theta}^T} & \cdots & \frac{\partial\mathbf{a}(\boldsymbol{\theta}_D)}{\partial\boldsymbol{\theta}^T}\end{array}\right]^H\boldsymbol{\Pi}^{\perp}_{\mathbf{A}(\boldsymbol{\Theta})}\\ &\qquad\times\left[\begin{array}{ccc}\frac{\partial\mathbf{a}(\boldsymbol{\theta}_1)}{\partial\boldsymbol{\theta}^T} & \cdots & \frac{\partial\mathbf{a}(\boldsymbol{\theta}_D)}{\partial\boldsymbol{\theta}^T}\end{array}\right],\end{aligned} \tag{3}$$

where $\mathbf{F}_{\boldsymbol{\Theta}}$ is the Fisher information matrix (FIM), $\odot$ denotes the Hadamard product, $\otimes$ denotes the Kronecker product, and $\widehat{\mathbf{R}}_{\mathbf{s}} = \frac{1}{T}\sum_{t=1}^{T}\mathbf{s}_t\mathbf{s}_t^H$. In this contribution we are interested in the single source case ($D = 1$), where

$$\mathbf{x}_t = \mathbf{a}\left(\boldsymbol{\theta}\right)s_t + \mathbf{n}_t,\ 1 \leq t \leq T. \tag{4}$$

$$\widehat{\boldsymbol{\theta}} = \arg\left\{\max_{\boldsymbol{\theta}}\left\{\sum_{t=1}^{T}\mathbf{x}_t^H\boldsymbol{\Pi}_{\mathbf{a}(\boldsymbol{\theta})}\mathbf{x}_t\right\}\right\}, \tag{5}$$

and the FIM is $\mathbf{F}_{\boldsymbol{\theta}} = \frac{2T}{\sigma^2}\mathrm{Re}\left\{\boldsymbol{\Phi}\left(\boldsymbol{\theta}\right)\odot\left(\widehat{\sigma_s^2}\otimes\mathbf{1}_{P,P}\right)\right\}$, with $\boldsymbol{\Phi}\left(\boldsymbol{\theta}\right) = \frac{\partial\mathbf{a}(\boldsymbol{\theta})}{\partial\boldsymbol{\theta}^T}^H\boldsymbol{\Pi}^{\perp}_{\mathbf{a}(\boldsymbol{\theta})}\frac{\partial\mathbf{a}(\boldsymbol{\theta})}{\partial\boldsymbol{\theta}^T}$ and $\widehat{\sigma_s^2} = \frac{1}{T}\sum_{t=1}^{T}\left|s_t\right|^2$. Therefore, $\mathbf{CRB}_{\boldsymbol{\theta}} = \mathbf{F}_{\boldsymbol{\theta}}^{-1}$, is computed from

$$\mathbf{F}_{\boldsymbol{\theta}} = \frac{2}{\sigma^2}\left(\sum_{t=1}^{T}\left|s_t\right|^2\right)\left(\frac{\partial\mathbf{a}\left(\boldsymbol{\theta}\right)}{\partial\boldsymbol{\theta}^T}^H\boldsymbol{\Pi}^{\perp}_{\mathbf{a}(\boldsymbol{\theta})}\frac{\partial\mathbf{a}\left(\boldsymbol{\theta}\right)}{\partial\boldsymbol{\theta}^T}\right). \tag{6}$$

B. Coherent Processing

Considering T received signal observations, the so-called coherent signal model can be written as

$$\begin{aligned}&\begin{array}{c}\mathbf{x}_1 = \mathbf{a}\left(\boldsymbol{\theta}\right)s + \mathbf{n}_1\\ \vdots\\ \mathbf{x}_T = \mathbf{a}\left(\boldsymbol{\theta}\right)s + \mathbf{n}_T\end{array} \Leftrightarrow \begin{pmatrix}\mathbf{x}_1\\ \vdots\\ \mathbf{x}_T\end{pmatrix} = \begin{pmatrix}\mathbf{a}\left(\boldsymbol{\theta}\right)\\ \vdots\\ \mathbf{a}\left(\boldsymbol{\theta}\right)\end{pmatrix}s + \begin{pmatrix}\mathbf{n}_1\\ \vdots\\ \mathbf{n}_T\end{pmatrix}\\ &\Leftrightarrow\left\{\begin{array}{c}\underline{\mathbf{x}}_T = \underline{\mathbf{a}}\left(\boldsymbol{\theta}\right)s + \underline{\mathbf{n}}_T\\ \underline{\mathbf{a}}\left(\boldsymbol{\theta}\right) = \mathbf{1}_{T,1}\otimes\mathbf{a}\left(\boldsymbol{\theta}\right)\end{array}\right..\end{aligned} \tag{7}$$

This model is valid as long as the received signal does not lose its coherency (i.e., constant phase) during the observation time (e.g., specular reflections or short observation times).

Then, the coherent MLE (superscript $(\cdot)^C$) of $\boldsymbol{\theta}$ (5) is

$$\widehat{\boldsymbol{\theta}}^C = \arg\left\{\max_{\boldsymbol{\theta}}\left\{\left|\frac{\underline{\mathbf{a}}\left(\boldsymbol{\theta}\right)^H\underline{\mathbf{x}}_T}{\left\|\underline{\mathbf{a}}\left(\boldsymbol{\theta}\right)\right\|}\right|^2\right\}\right\}, \tag{8}$$

and the coherent FIM (6) is written as (i.e., w.r.t. $\underline{\mathbf{a}}\left(\boldsymbol{\theta}\right)$)

$$\mathbf{F}_{\boldsymbol{\theta}}^C = \frac{2\left|s\right|^2}{\sigma^2}\left(\frac{\partial\underline{\mathbf{a}}\left(\boldsymbol{\theta}\right)}{\partial\boldsymbol{\theta}^T}^H\boldsymbol{\Pi}^{\perp}_{\underline{\mathbf{a}}(\boldsymbol{\theta})}\frac{\partial\underline{\mathbf{a}}\left(\boldsymbol{\theta}\right)}{\partial\boldsymbol{\theta}^T}\right). \tag{9}$$

If we further elaborate on the FIM computation,

$$\begin{aligned}&\frac{\partial\underline{\mathbf{a}}\left(\boldsymbol{\theta}\right)}{\partial\boldsymbol{\theta}^T}^H\boldsymbol{\Pi}^{\perp}_{\underline{\mathbf{a}}(\boldsymbol{\theta})}\frac{\partial\underline{\mathbf{a}}\left(\boldsymbol{\theta}\right)}{\partial\boldsymbol{\theta}^T} = \frac{\partial\underline{\mathbf{a}}\left(\boldsymbol{\theta}\right)}{\partial\boldsymbol{\theta}^T}^H\frac{\partial\underline{\mathbf{a}}\left(\boldsymbol{\theta}\right)}{\partial\boldsymbol{\theta}^T}\\ &-\frac{1}{\underline{\mathbf{a}}\left(\boldsymbol{\theta}\right)^H\underline{\mathbf{a}}\left(\boldsymbol{\theta}\right)}\left(\frac{\partial\underline{\mathbf{a}}\left(\boldsymbol{\theta}\right)}{\partial\boldsymbol{\theta}^T}^H\underline{\mathbf{a}}\left(\boldsymbol{\theta}\right)\right)\left(\frac{\partial\underline{\mathbf{a}}\left(\boldsymbol{\theta}\right)}{\partial\boldsymbol{\theta}^T}^H\underline{\mathbf{a}}\left(\boldsymbol{\theta}\right)\right)^H\\ &= T\frac{\partial\mathbf{a}\left(\boldsymbol{\theta}\right)}{\partial\boldsymbol{\theta}^T}^H\frac{\partial\mathbf{a}\left(\boldsymbol{\theta}\right)}{\partial\boldsymbol{\theta}^T}\\ &-\frac{1}{T\mathbf{a}\left(\boldsymbol{\theta}\right)^H\mathbf{a}\left(\boldsymbol{\theta}\right)}\left(T\frac{\partial\mathbf{a}\left(\boldsymbol{\theta}\right)}{\partial\boldsymbol{\theta}^T}^H\mathbf{a}\left(\boldsymbol{\theta}\right)\right)\left(T\frac{\partial\mathbf{a}\left(\boldsymbol{\theta}\right)}{\partial\boldsymbol{\theta}^T}^H\mathbf{a}\left(\boldsymbol{\theta}\right)\right)^H\\ &= T\frac{\partial\mathbf{a}\left(\boldsymbol{\theta}\right)}{\partial\boldsymbol{\theta}^T}^H\boldsymbol{\Pi}^{\perp}_{\mathbf{a}(\boldsymbol{\theta})}\frac{\partial\mathbf{a}\left(\boldsymbol{\theta}\right)}{\partial\boldsymbol{\theta}^T}.\end{aligned}$$

Therefore, the coherent processing FIM is

$$\mathbf{F}_{\boldsymbol{\theta}}^C = \frac{2T\left|s\right|^2}{\sigma^2}\left(\frac{\partial\mathbf{a}\left(\boldsymbol{\theta}\right)}{\partial\boldsymbol{\theta}^T}^H\boldsymbol{\Pi}^{\perp}_{\mathbf{a}(\boldsymbol{\theta})}\frac{\partial\mathbf{a}\left(\boldsymbol{\theta}\right)}{\partial\boldsymbol{\theta}^T}\right). \tag{10}$$

C. Non-Coherent Processing

Considering again the complete received signal observation time T, the so-called non-coherent signal model (i.e., when the signal complex amplitude can not be considered constant during the observation time) is written as

$$\left\{\ \mathbf{x}_1 = \mathbf{a}\left(\boldsymbol{\theta}\right)s_1 + \mathbf{n}_1, \cdots, \mathbf{x}_T = \mathbf{a}\left(\boldsymbol{\theta}\right)s_T + \mathbf{n}_T\ \right. . \tag{11}$$

In this case, the non-coherent MLE (superscript $(\cdot)^{NC}$) of $\boldsymbol{\theta}$, is given by the single source MLE in (5), and the non-coherent FIM is given by the single source FIM expression in (6)

$$\widehat{\boldsymbol{\theta}}^{NC} = \arg\left\{\max_{\boldsymbol{\theta}}\left\{\sum_{t=1}^{T}\left|\frac{\mathbf{a}\left(\boldsymbol{\theta}\right)^H\mathbf{x}_t}{\left\|\mathbf{a}\left(\boldsymbol{\theta}\right)\right\|}\right|^2\right\}\right\}, \tag{12}$$

$$\mathbf{F}_{\boldsymbol{\theta}}^{NC} = \frac{2}{\sigma^2}\left(\sum_{t=1}^{T}\left|s_t\right|^2\right)\left(\frac{\partial\mathbf{a}\left(\boldsymbol{\theta}\right)}{\partial\boldsymbol{\theta}^T}^H\boldsymbol{\Pi}^{\perp}_{\mathbf{a}(\boldsymbol{\theta})}\frac{\partial\mathbf{a}\left(\boldsymbol{\theta}\right)}{\partial\boldsymbol{\theta}^T}\right). \tag{13}$$

Lemma 1: In the case of iso-energy received signals, $\sum_{t=1}^{T}\left|s_t\right|^2 = T\left|s\right|^2$ (e.g., for the direct GNSS signal or in case of specular reflections), then the FIM in (13) *reduces to*

$$\mathbf{F}_{\boldsymbol{\theta}}^{NC} = \frac{2T\left|s\right|^2}{\sigma^2}\left(\frac{\partial\mathbf{a}\left(\boldsymbol{\theta}\right)}{\partial\boldsymbol{\theta}^T}^H\boldsymbol{\Pi}^{\perp}_{\mathbf{a}(\boldsymbol{\theta})}\frac{\partial\mathbf{a}\left(\boldsymbol{\theta}\right)}{\partial\boldsymbol{\theta}^T}\right) = \mathbf{F}_{\boldsymbol{\theta}}^C, \tag{14}$$

which in turn implies that the corresponding CRBs for both single source coherent and non-coherent processing schemes are equivalent (i.e., not the case for multiple sources).

Notice that both system models (7) and (11) are particular instances of the general CSM, and therefore, the MLE of $\boldsymbol{\theta}$ and $(s_1, \ldots, s_T)$ are known to be asymptotically efficient, i.e., optimal in the large sample regime and/or high SNR regime of the CSM [12], [13].

D. Coherent and Non-Coherent Estimators

The fully coherent and non-coherent estimators in (8) and (12) are the two limiting cases of the class of PDI techniques, but other approaches exist [15]. Let us first define a given generic estimator as $\hat{\boldsymbol{\theta}} = \arg\{\max_{\boldsymbol{\theta}} \{\mathcal{L}(\underline{\mathbf{x}}_T)\}\}$, with T the total number of observations, as well as $y_k = \frac{\underline{\mathbf{a}}(\boldsymbol{\theta})^H \underline{\mathbf{x}}_k}{\|\underline{\mathbf{a}}(\boldsymbol{\theta})\|}$, $\underline{\mathbf{x}}_k^T = (\mathbf{x}_{(k-1)T_c+1}^T, \ldots, \mathbf{x}_{kT_c}^T)$, the output of the coherent matched filter for T_c observations, $T = N_{nc}T_c$, and N_{nc} the number of non-coherent combinations. We consider the following estimators:

- Coherent processing: $\mathcal{L}_C(\underline{\mathbf{x}}_T) = \left|\sum_{k=1}^{N_{nc}} y_k\right|^2$
- Non-coherent processing: $\mathcal{L}_{NC}(\underline{\mathbf{x}}_T) = \sum_{k=1}^{N_{nc}} |y_k|^2$
- Non-quadratic non-coherent: $\mathcal{L}_{NQNC}(\underline{\mathbf{x}}_T) = \sum_{k=1}^{N_{nc}} |y_k|$
- Non-coherent squaring detector [23]: $\mathcal{L}_{NCSD}(\underline{\mathbf{x}}_T) = \sum_{k=1}^{N_{nc}} |y_k|^2 + \left|\sum_{k=1}^{N_{nc}} y_k^2\right|$

Notice that the results presented in Sec. III are valid for any coherent/non-coherent combination. Also, in order to eliminate a possible antenna crosstalk/multipath, it was proposed in [18] to subtract the coherent part of signal, which is not discussed.

III. Validation and Discussion

To validate the previous theoretical result (i.e., coherent and non-coherent CRBs are equivalent for coherent signals), and provide insights on the estimation performance of the non-coherent GNSS-R processing, we consider the schemes in Sec. II-D for two GNSS-R altimetry estimation problems [3], [4]: 1) Direct and reflected signals have the same Doppler, which can be compensated from the direct signal processing); and 2) Direct and reflected signals have different Dopplers, and both delay and Doppler must be estimated.

A. Generic GNSS Signal Model

We consider the transmission of a band-limited GNSS signal $s(t)$ with sampling frequency F_s over a carrier with frequency f_c, from a transmitter T at position $\mathbf{p}_T(t)$ to a receiver R at position $\mathbf{p}_R(t)$, in uniform linear motion. The propagation delay, $\tau(t)$, during the observation time, can be approximated by a 1st order distance-velocity model, $\|\mathbf{p}_{TR}(t)\| \triangleq \|\mathbf{p}_T(t - \tau(t)) - \mathbf{p}_R(t)\| = c\tau(t) \simeq d + vt$, $\tau(t) \simeq \tau + bt$, $\tau = \frac{d}{c}$, $b = \frac{v}{c}$, where d is the T-to-R relative radial distance, v the T-to-R relative radial velocity, b a delay drift related to the Doppler effect, and the unknown parameters to be estimated $\boldsymbol{\eta}^T = [\tau, b]$. Considering the narrowband signal assumption, a good approximation of the receiver's Hilbert filter output is,

$$x(t) = \alpha e^{-j2\pi f_c b(t-\tau)} s(t-\tau) + n(t), \tag{15}$$

with $n(t)$ a complex white circular Gaussian noise within the filter bandwidth with unknown variance σ_n^2, and α a complex gain. The discrete vector signal model is build from $N = N_1 + N_2 + 1$ samples at $T_s = 1/F_s$,

$$\begin{aligned} &\mathbf{x} = \alpha \mathbf{a}(\boldsymbol{\eta}) + \mathbf{n} = \rho e^{j\varphi} \mathbf{a}(\boldsymbol{\eta}) + \mathbf{n}, \\ &\mathbf{x} = (\ldots, x(kT_s), \ldots)^\top, \mathbf{n} = (\ldots, n(kT_s), \ldots)^\top, \\ &\mathbf{a}(\boldsymbol{\eta}) = (\ldots, s(kT_s - \tau) e^{-j2\pi f_c (b(kT_s - \tau)}, \ldots)^\top, \end{aligned} \tag{16}$$

with $N_1 \leq k \leq N_2$ and $\mathbf{n} \sim \mathcal{CN}\left(\mathbf{0}, \sigma_n^2 \mathbf{I}_N\right)$. The unknown deterministic parameters can be gathered in vector $\boldsymbol{\epsilon} = \left(\sigma_n^2, \rho, \varphi, \tau, b\right)^\top$, with $\alpha = \rho e^{j\varphi}$ ($\rho \in \mathbb{R}^+$, $0 \leq \varphi \leq 2\pi$). The closed-form CRB expression associated to the estimation of $\boldsymbol{\epsilon}$ for the signal model (16) was recently released in [24].

The previous GNSS signal model (15)-(16) is valid for any signal. We consider a GPS L1 C/A signal with a PRN code length 1023 chips and with a chip rate of 1.023 MHz. Recall that the bit period is 20 ms, which is not an issue if the bit transitions are properly handled (i.e., data wipe-off). For the coherent processing we use 20 ms of signal, that is, 20 consecutive PRN codes. For the non-coherent schemes we use $N_{nc} = 20$ blocks of 1 ms.

Indeed, the coherent time limit is because of the T-to-R relative movement and the size of the first Fresnel zone (1FZ) (i.e., 300-500 m). As stated in [19], most GNSS reflected power comes from 0.6 times the size of such 1FZ, thus considering 300 m leads to 180 m for most of the reflected power, which translates to 25 ms of integration at Low Earth Orbit (LEO).

B. Code-based Conventional GNSS-R Altimetry

In the following results the performance metric is the root mean square error (RMSE) on the delay, phase and Doppler estimates. The results presented are generic, so no specific type of platform is assumed, therefore being valid for ground-based, airborne or spaceborne specular reflection coherent scenarios.

1) Results for Time-delay and Phase Estimation: in GNSS-R altimetry, the main parameter of interest is the reflected signal delay. We consider first that the Doppler is perfectly compensated from the direct signal processing, then (15) reduces to $x(t) = \rho e^{j\varphi} s(t-\tau) + n(t)$, and the parameters to be estimated are $\boldsymbol{\epsilon} = \left(\sigma_n^2, \rho, \varphi, \tau\right)^\top$. In this case, the coherent and non-coherent signal models coincide with (7) and (11), and for the delay estimation the theoretical result in Sec. II holds. RMSE delay estimation results w.r.t. the SNR at the output of the coherent matched filter, for the different schemes in Sec. II-D, are shown in Fig. 1 (top). We can see that all estimators reach the CRB (i.e., they are efficient), and only the threshold region varies. The latter implies that for non-coherent schemes a slightly larger SNR is needed to be in the optimal operation regime. This validates the theoretical result in Lemma 1, and it implies that for long enough averaging the GNSS-R non-coherent processing is optimal.

In addition, for precise GNSS-R altimetry the practitioner may want to use carrier phase measurements [4]–[6]. Notice that non-coherent processing schemes are designed to get rid of phase changes, but we can still compare the coherent/non-coherent phase estimation performance by computing the

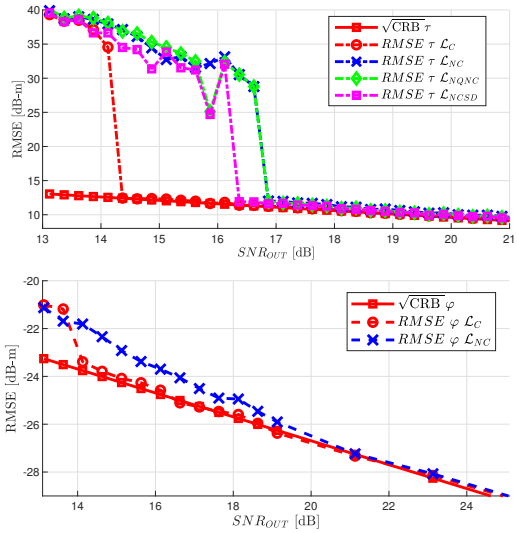

Fig. 1. (Top) Delay CRB/RMSE and (Bottom) phase CRB/RMSE for different coherent/non-coherent combination schemes and $F_s = 2.046$ MHz.

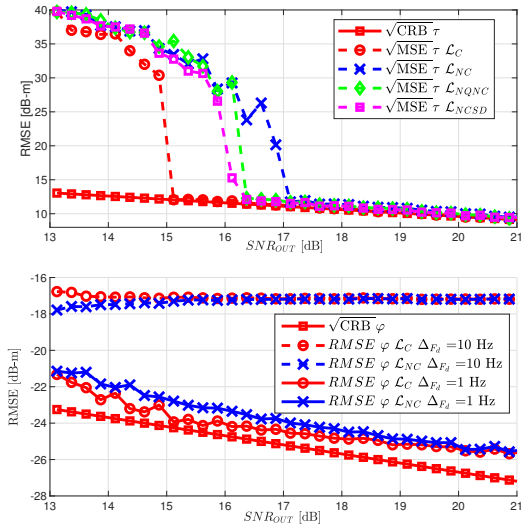

Fig. 2. (Top) Delay CRB/RMSE and (Bottom) phase CRB/RMSE for the misspecified Doppler compensation case, and $F_s = 2.046$ MHz.

RMSE of (with τ^C the coherent time-delay estimate and τ_k^{NC} the non-coherent one for each processing block):

$$\widehat{\varphi}^C = \arg\left\{\sum_{k=1}^{N_{nc}} y_k(\widehat{\tau}^C)\right\};\ \widehat{\varphi}^{NC} = \frac{1}{N_{nc}}\sum_{k=1}^{N_{nc}} \arg\left\{y_k(\widehat{\tau}_k^{NC})\right\}$$

Results for the phase are shown in Fig. 1 (bottom), where we see that both $\widehat{\varphi}^C$ and $\widehat{\varphi}^{NC}$ RMSE converge to the phase CRB, and the difference is again in the threshold region. This was expected as the phase MLE is the argument of the cross-ambiguity function evaluated at the delay estimate, then, when the delay estimate converged, so does the phase estimate.

2) Impact of a Misspecified Doppler Wipe-off in Time-delay and Phase Estimation: because the direct signal processing Doppler is an estimate of the true one, it is wise to assess the impact of a Doppler misspecification. The signal model is

$$x(t) = \rho e^{j\varphi} s(t-\tau)\, e^{-j2\pi f_c \Delta b (t-\tau)} + n(t), \qquad (17)$$

with the residual Doppler error $f_c\Delta b = f_c(b - \widehat{b})$. This is a misspecified signal model and we estimate $\boldsymbol{\epsilon}^\top = \left(\sigma_n^2, \rho, \varphi, \tau\right)$, as if $\Delta b = 0$, while the true error $\Delta b \neq 0$. Results for $\Delta F_d = f_c\Delta b = \{1, 10\}$ Hz are shown in Fig. 2 (refer to Fig. 3 (middle plot) for the Doppler error range in the asymptotic regime, RMSE = [0-6] dB which translate to $[-3\sigma, 3\sigma]$ equal to [-3,3] Hz and [-12,12] Hz), where we can see that the different delay estimators still converge to the CRB despite of the misspecified Doppler compensation. This result further supports that the non-coherent schemes are optimal regardless of the Doppler estimation precision (i.e., in the asymptotic regime). In contrast, the phase estimates do not converge to the CRB, and may be useless if not accounting for the Doppler.

C. Joint Time-delay, Doppler and Phase Estimation

We consider now the case where the Doppler is not the same for the direct and reflected signals. The joint delay, Doppler and phase estimation must be considered to cope with situations where different reflected Dopplers coming from different places of the Glistening zone appear, for which the approach in Sec. III-B is no longer valid. In this case the signal model is the one in (15), and the parameters to be estimated are $\boldsymbol{\epsilon}^\top = \left(\sigma_n^2, \rho, \varphi, \tau, b\right)$. Because of the Doppler effect, the coherent and non-coherent signal models do not coincide, and therefore, the result in Sec. II does no longer hold. But carefully analyzing the CRB we can see that for real GNSS signals the delay and Doppler estimation is decoupled [24] (i.e., the off-diagonal terms of the CRB matrix are zero). Therefore, we can still validate the performance degradation of the different non-coherent schemes in Sec. II-D w.r.t. the optimal coherent one. Results are shown in Fig. 3.

The delay estimation (Fig. 3 (top)) converges again to the CRB for all the schemes, and we obtain the same results and conclusions as in the previous scenarios. Regarding the phase estimation (Fig. 3 (bottom)), there is a clear difference between the coherent and non-coherent schemes. While the former converges the latter does not. This is mainly because of the performance degradation of the non-coherent Doppler estimate, which is shown in Fig. 3 (middle), and is about 13 dB w.r.t. the optimal, except for the NCSD. Indeed, the NCSD is the only scheme which converges to the coherent processing Doppler CRB, because is the one that captures both the coherent and the incoherent part of the GNSS signal. Therefore, the NCSD is the non-coherent processing to be used for a correct Doppler estimation.

IV. Conclusion

The goal of this contribution was to provide new insights on the achievable estimation performance of coherent/non-coherent processing schemes in GNSS-R, by comparing the MLE performance to the corresponding CRB. First, it was theoretically shown that for certain CSMs (i.e., iso-energy received signals), both coherent and non-coherent CRBs are equivalent, then for these models any coherent/non-coherent

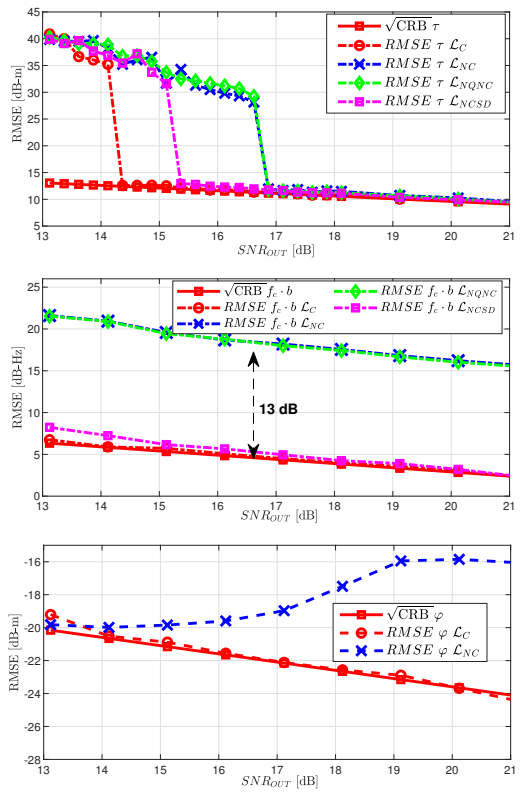

Fig. 3. (Top) Delay CRB/RMSE, (Middle) Doppler CRB/RMSE and (Bottom) phase CRB/RMSE, for $F_s = 2.046$ MHz.

combination MLE is optimal at high SNR. This equivalence depends on both the scenario and the parameters to be estimated, a subtle result with strong practical implications. Indeed, the equivalence was first validated for a set of representative non-coherent estimation schemes in a conventional GNSS-R altimetry delay estimation problem, considering both a perfect and misspecified Doppler wipe-off. In this case it was shown that the non-coherent delay estimation is asymptotically optimal as long as the direct signal Doppler estimate is in its asymptotic regime. The analysis was then extended to the more general joint delay, Doppler and phase estimation problem considering different direct and reflected signal Dopplers. For instance, to cope with the situation where different reflected Dopplers are coming from different places of the Glistening zone. In general, using GNSS signals, the non-coherent delay estimation is asymptotically efficient regardless of the Doppler estimation performance, which in turn is only optimal for a specific scheme using the squaring detector, being the one that captures both the coherent and the incoherent part of the GNSS signal. Therefore, the standard GNSS-R altimetry processing is optimal but more sophisticated algorithms must be accounted for to optimally use the signal carrier Doppler and phase information.

REFERENCES

[1] P. J. G. Teunissen and O. Montenbruck, Eds., *Handbook of Global Navigation Satellite Systems*. Switzerland: Springer, 2017.

[2] H. L. Van Trees, *Detection, Estimation, and Modulation Theory, Part III: Radar – Sonar Signal Processing and Gaussian Signals in Noise*. John Wiley & Sons, 2001.

[3] V. U. Zavorotny, S. Gleason, E. Cardellach, and A. Camps, "Tutorial on Remote Sensing using GNSS Bistatic Radar of Opportunity," *IEEE Geosci. Remote Sens. Mag.*, vol. 2, no. 4, pp. 8–45, Dec. 2014.

[4] L. Lestarquit *et al.*, "Reflectometry With an Open-Source Software GNSS Receiver: Use Case With Carrier Phase Altimetry," *IEEE Journal of Selected Topics in Applied Earth Observations and Remote Sensing*, vol. 9, no. 10, pp. 4843–4853, Oct. 2016.

[5] W. Li, , E. Cardellach, F. Fabra, A. Rius, S. Ribó, and M. Martín-Neira, "First Spaceborne Phase Altimetry Over Sea Ice Using TechDemoSat-1 GNSS-R Signals," *Geophys. Res. Lett.*, vol. 44, no. 16, 2017.

[6] E. Cardellach, W. Li, A. Rius, M. Semmling, J. Wickert, F. Zus, C. S. Ruf, and C. Buontempo, "First Precise Spaceborne Sea Surface Altimetry With GNSS Reflected Signals," *IEEE J. Select. Topics Appl. Earth Observ. Remote Sensing*, vol. 13, pp. 102–112, 2019.

[7] A. Camps *et al.*, "Sensitivity of GNSS-R Spaceborne Observations to Soil Moisture and Vegetation," *IEEE J. Sel. Top. Appl. Earth Obs. Remote Sens.*, vol. 9, no. 10, pp. 4730–4742, Oct. 2016.

[8] D. Pascual *et al.*, "Simulation and Analysis of GNSS-R Composite Waveforms Using GPS and Galileo Signals," *IEEE J. Sel. Topics Appl. Earth Observ.*, vol. 7, no. 5, pp. 1461–1468, May 2014.

[9] E. Cardellach *et al.*, "Consolidating the Precision of Interferometric GNSS-R Ocean Altimetry Using Airborne Experimental Data," *IEEE Trans. Geosci. Remote Sens.*, vol. 52, no. 8, pp. 4992–5004, Aug. 2014.

[10] W. Li, A. Rius, F. Fabra, E. Cardellach, S. Ribó, and M. Martín-Neira, "Revisiting the GNSS-R Waveform Statistics and Its Impact on Altimetric Retrievals," *IEEE Trans. Geosci. Remote Sens.*, vol. 56, no. 5, pp. 2854–2871, May 2018.

[11] H. L. Van Trees, K. L. Bell, and Z. Tian, *Detection, Estimation and Modulation Theory - Part 1*, 2nd ed. Wiley, 2013.

[12] P. Stoica and A. Nehorai, "Performances Study of Conditional and Unconditional Direction of Arrival Estimation," *IEEE Trans. Acoust., Speech, Signal Process.*, vol. 38, no. 10, pp. 1783–1795, Oct. 1990.

[13] A. Renaux, P. Forster, E. Chaumette, and P. Larzabal, "On the High-SNR Conditional Maximum-Likelihood Estimator Full Statistical Characterization," *IEEE Trans. Signal Process.*, vol. 54, no. 12, pp. 4840 – 4843, Dec. 2006.

[14] D. Borio, C. O'Driscoll, and G. Lachapelle, "Coherent, Noncoherent, and Differentially Coherent Combining Techniques for Acquisition of New Composite GNSS Signals," *IEEE Trans. Aerosp. Electron. Syst.*, vol. 45, no. 3, pp. 1227–1240, July 2009.

[15] D. Gomez-Casco, J. A. Lopez-Salcedo, and G. Seco-Granados, "Optimal Post-Detection Integration Techniques for the Reacquisition of Weak GNSS Signals," *IEEE Trans. Aerosp. Electron. Syst.*, vol. 56, no. 3, pp. 2302–2311, June 2020.

[16] E. Valencia *et al.*, "Experimental Determination of the Sea Correlation Time Using GNSS-R Coherent Data," *IEEE Geosci. Remote. Sens. Lett.*, vol. 7, no. 4, pp. 675–679, Oct. 2010.

[17] H. Park *et al.*, "Analysis of Spaceborne GNSS-R Delay-Doppler Tracking," *IEEE J. Sel. Topics Appl. Earth Observ.*, vol. 7, no. 5, pp. 1481–1492, May 2014.

[18] F. Martin *et al.*, "Mitigation of Direct Signal Cross-Talk and Study of the Coherent Component in GNSS-R," *IEEE Geosci. Remote. Sens. Lett.*, vol. 12, no. 2, pp. 279–283, Feb. 2015.

[19] A. Camps, "Spatial Resolution in GNSS-R Under Coherent Scattering," *IEEE Geosci. Remote. Sens. Lett.*, vol. 17, no. 1, pp. 32–36, Jan. 2020.

[20] J. F. Munoz-Martin *et al.*, "Untangling the Incoherent and Coherent Scattering Components in GNSS-R and Novel Applications," *Remote Sensing*, vol. 12, no. 7, 2020.

[21] B. Ottersten, M. Viberg, P. Stoica, and A. Nehorai, "Exact and Large Sample Maximum Likelihood Techniques for Parameter Estimation and Detection in Array Processing," in *Radar Array Processing*, S. Haykin, J. Litva, and T. J. Shepherd, Eds. Heidelberg: Springer-Verlag, 1993, ch. 4, pp. 99–151.

[22] S. F. Yau and Y. Bresler, "A Compact Cramér-Rao Bound Expression for Parametric Estimation of Superimposed Signals," *IEEE Trans. Signal Process.*, vol. 40, no. 5, pp. 1226–1230, May 1992.

[23] D. Borio, "Non-Coherent Squaring Detector and Its Application to Bi-Phased Signals," *IET Radar, Sonar & Navigation*, vol. 8, no. 4, pp. 327–335, April 2014.

[24] D. Medina, L. Ortega, J. Vilà-Valls, P. Closas, F. Vincent, and E. Chaumette, "Compact CRB for Delay, Doppler and Phase Estimation - Application to GNSS SPP & RTK Performance Characterization," *IET Radar, Sonar Navig.*, vol. 14, no. 10, pp. 1537–1549, 2020.